Structural Engineering and Mechanics, *Vol. 52, No. 1 (2014) 35-49*
DOI: http://dx.doi.org/10.12989/sem.2014.52.1.035

A study of deterioration of reinforced concrete beams under various forms of simulated acid rain attack in the laboratory

Yingfang Fan*[1], Zhiqiang Hu[2], Haiyang Luan[1], Dawei Wang[1] and An Chen[3]

[1]*Institute of Road and Bridge Engineering, Dalian Maritime University, Dalian 116026, China*
[2]*School of Hydraulic Engineering, Dalian University of Technology, Dalian 116023, China*
[3]*Department of Civil Engineering, University of Idaho, Idaho 441022, USA*

(Received October 31, 2012, Revised May 14, 2014, Accepted May 18, 2014)

Abstract. This paper studies the behaviour of deteriorated reinforced concrete (RC) beams attacked by various forms of simulated acid rain. An artificial rainfall simulator was firstly designed and evaluated. Eleven RC beams (120 mm×200 mm×1800 mm) were then constructed in the laboratory. Among them, one was acting as a reference beam and the others were subjected to three accelerated corrosion methods, including immersion, wetting-drying, and artificial rainfall methods, to simulate the attack of real acid rain. Acid solutions with pH levels of 1.5 and 2.5 were considered. Next, ultrasonic, scanning electron microscopy (SEM), dynamic, and three-point bending tests were performed to investigate the mechanical properties of concrete and flexural behaviour of the RC beams. It can be concluded that the designed artificial simulator can be effectively used to simulate the real acid rainfall. Both the immersion and wetting-drying methods magnify the effects of the real acid rainfall on the RC beams.

Keywords: acid deposition; reinforced concrete beam; deterioration; flexural strength; corrosion depth

1. Introduction

Acid rain is a serious environmental problem that affects large parts of the world (Neuman 1985, Eney *et al.* 1987, Mansfeld *et al.*1988, Larssen *et al.*1999, Chen *et al.* 2013), and it typically has a pH value less than 5.7, which contains strongly aggressive agents (e.g., sulfuric acid, nitric acid, etc.) (Berner *et al.* 1996). Presently, North Europe acid rain area, North American acid rain area and Chinese acid rain area are the three main acid rain areas in the world. In China, the acid rain falls have covered at least one third of territory (Zhao 2006, Zhang *et al*. 2010, Zhang *et al.* 2012, Grismer 2012). In Wheeling, West Virginia, rainfall at a pH value of 1.5 was once measured (Keller 2012). In cities around the world, large amounts of irreplaceable statues and infrastructural facilities (i.e., bridges, buildings, etc.) have been significantly damaged by acid deposit; resulting in losses of billions of dollars per year (Keller 2012). In order to ensure the durability of concrete structures servicing in the acid rain environment, damage mechanism and process of reinforced concrete (RC) structures attacked by acid rain need to be understood, which is the motivation of this study.

*Corresponding author, Professor, E-mail: fanyf72@aliyun.com

http://www.techno-press.org/?journal=sem&subpage=8 ISSN: 1225-4568 (Print), 1598-6217 (Online)

In past studies, corroded RC specimens can be divided into two groups: (1) accelerated corroded specimens, which are corroded by accelerated corrosion methods in the laboratory, such as current, spraying aggressive agent, etc. (O'Flaherty *et al.* 2008, Ababneh *et al.* 2011, Zhou *et al.* 2011), and (2) in-situ specimens, which are delivered directly from the field. These specimens have been in service for a certain time in the actual aggressive environment and are severely corroded (Fan *et al.* 2005, Francois *et al.* 2013). Since it takes much longer time for the in-situ specimens to reach the same level of corrosion comparing to the accelerated corroded specimens, accelerated corrosion methods have been widely used to study the behavior of the reinforced concrete specimens exposed to severe environment. Immersion, wetting-drying, and electrochemical methods are three traditional accelerating methods (Belie *et al.* 2002). More recently, in the research fields of agriculture and soil protection, rainfall simulators have been developed to simulate the rainfall in the laboratory (Laws 1941, Fan *et al.*1991, Xu *et al.* 2006, Sangüesa *et al.* 2010). It was reported that rainfall simulators can more accurately represent the environmental condition. However, to use this apparatus to simulate acid rainfall has not been reported. Therefore, an artificial rainfall simulator was designed and evaluated in this study. Together with immersion and wetting-drying methods, it was used to corrode large-scale RC beams constructed in the laboratory. The acid solutions with pH level 1.5 and 2.5 were considered. After being exposed to the simulated environments, nondestructive and three-point bending tests were carried out to evaluate the damage state of concrete and flexural behavior of the RC beams, respectively. The results from different simulated methods are obtained and compared.

2. Research significance

The objective of this paper is to evaluate damage evolutions of RC beams servicing in acid rain environment. To achieve accelerated corrosion, accelerated corrosion system needs to be constructed in the laboratory. Currently, electronic chemical accelerated system, and immersion or wetting-drying using corrosive solutions are major accelerated corrosion systems that have been widely accepted. However, the coupled effects of corrosion and rainfall are neglected from these studies. In addition, it is unclear whether the simulated corrosive environments can accurately reflect the real condition. Recently, there were some research focused on the damage mechanism and mechanical properties of cement, mortar and concrete exposed to the acid rain (Okochi *et al.* 2000, Xie *et al.* 2004, Fan *et al.* 2010, Fan *et al.* 2012, Chen *et al*. 2013). However, up to now, little research work was focused on mechanical behavior of reinforced concrete beams under the effect of acid rainfall. Therefore, as an important step further, an artificial rainfall simulator was designed in this study, which can take both the loading and chemical effects of acid rainfall into consideration. The effects of acid rainfall simulator are compared with two other accelerated methods (immersion and wetting-drying) on the behavior of RC beams.

3. Design of the rainfall simulator

To simulate the acid rainfall in the laboratory, an artificial rain deposition simulator was firstly designed in this paper (Fan *et al.* 2012).

3.1 Design of the rainfall simulator

The designed simulator consists of four parts: frame, container, rainfall system, and cyclic system, as shown in Fig. 1.

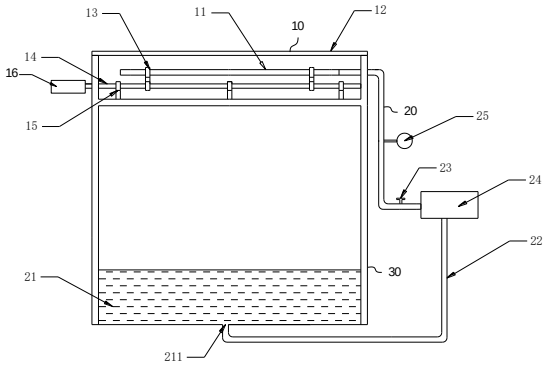

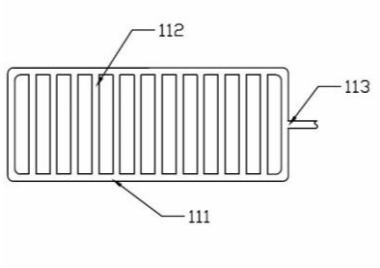

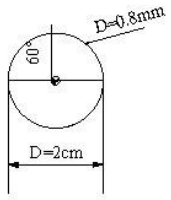

(1) design plot (2) detail of 11 (3) Spraying hole

Notes: 10: rainfall system; 11: rainfall plate; 12: reflect plate; 13: plate; 14: screw; 15: supporting plate; 16: controlled motor; 20: cyclic system; 21: water container; 22: main inlet pipe; 23: control valve; 24: centrifugal pump; 25: pressure gauge; 30: support; 111: inlet pipe; 112: spraying pipe; 113: water outlet; 211: water outlet

(a) design plot of the simulator

(b) Overview of the rainfall system

(c) Raining system

(f) Pressure meter

(g) Water inlet valve

(e) Water pump

Fig. 1 The designed rainfall simulator

3.1.1 Frame

The 3.5 m high frame is made of square steel. This height is required by the specific simulation condition. To mitigate corrosion of the steel, the surface of the steel frame is protected with an anti-corrosive coating.

3.1.2 Container

A rectangular container with a section of 50 cm×220 cm is made using PVC plates. Acid solutions are used in the cyclic system. Drainage and filtration system are mounted at the mid-bottom of the container.

3.1.3 Sprinklers

The raining system includes inlet pipes, spraying pipes, and a reflection plate. The dimension of the rainfall board is 212 cm×73 cm. The spraying pipes are 70 cm long and spaced at 10 cm on center. The reflection plate is 8.5 cm above the rainfall board. Both the inlet and spraying pipes are made of PVC, with diameters of 3.0 cm and 2.0 cm, respectively. To ensure the uniformity and the raindrop velocities, spraying holes with a diameter of 0.8 mm is drilled along the direction of right top 60 degree. Series of spraying holes are drilled every 10 cm along the length of the spraying pipes.

3.1.4 Cyclic system

Centrifugal pump, with the flow rate of two tons per hour and liftoff 25 m, is used to control the intensity of the rainfall. Pressure gauge and feed valve are used to control the intensity of the rainfall.

3.2 Evaluation of the rainfall simulator

The rainfall simulator was evaluated in the laboratory under a constant working pressure for: 1) homogeneity of rainfall, 2) intensity, 3) raindrop diameter, and 4) terminal velocity and kinetic energy. Tests were carried out for the sprinkler covering an area of 1900 mm×700 mm.

3.2.1 Homogeneity of simulated rainfall

Nine containers were put evenly in the rainfall area. The volumes of the raindrops falling in each container in one minute were measured, as shown in Table 1. It is calculated that the average coefficient of uniformity of the simulated rainfall is about 82%.

3.2.2 Rainfall intensity

For the purpose of accelerating the corrosion process, a heavy rainstorm was simulated in this paper. The flow amount of the centrifugal pump was two tons per hour, and the total rainfall in the area of 1900 mm × 700 mm was two tons. The rain intensity achieved was 4.18 mm/min.

Table 1 Volume of rain collected in the container

No	1	2	3	4	5	6	7	8	9
Volume /ml	95	91	82	70	71	65	57	55	50

3.2.3 Raindrop-size and splash velocity

In the simulated rain test, the raindrop diameter is usually measured by Filter paper splash method. If the raindrop velocity cannot achieve the terminal velocity, rotating disk or high-speed photography methods are typically used to measure the raindrop diameter. Since these methods are complex and difficult to implement, the physical model developed by Law (1941) as shown below was adopted in this study to calculate the raindrop diameter

$$V_T = 3.8 \ln D + 3.67 \tag{1}$$

where V_T is the terminal raindrop velocity, and D is the raindrop diameter. Based on previous studies (Park 1983, Wu 1995, Xu 2006), if the raindrop falls from the height of H (m) with an initial velocity of Vs, the splash velocity V_I can be calculated as

$$V_I = V_T \left[1 - \left(\frac{V_S}{V_T} \right) \exp\left(-2hH / {V_T}^2 \right) \right]^{\frac{1}{2}}, V_S = \frac{IA}{60 \times 10^3 A' N} \tag{2}$$

where I is the rainfall intensity (mm/min); A is the horizontal phasing control projected area of precipitation area; A' is the area of a single spraying hole; and N is the total numbers of the spraying holes.

In this study, the initial raindrop velocity was 1.16 m/s. The raindrop diameter was about 5 mm. From Eq. (2), it can be calculated that the terminal raindrop velocity was 9.8 m/s and the raindrop splash velocity was 9.5 m/s. Therefore, the raindrop splash velocity was close to the terminate velocity, which was in good agreement with reported data of real rainfall. The kinetic energy of an individual raindrop was 2.95×10^{-4} *J*.

3.3 Simulation of acid rain environment

Based on the constituent of the acid rain (Singh *et al*. 2008), a mixture of sulfate and nitric acid solutions was deposed to simulate the real rainfall environment. In this research, acidic solutions with pH level of 1.5 and 2.5 were deposed by mixing sulfate and nitric acid solutions (molar ratio is 9:1) in the laboratory. Acidity of the solution was recorded using a PB-10 Sartorius acidometer every twelve hours (Fig. 2).To keep the pH level of the solution constant, nitric acid was added to the solution periodically and mixed well with the solution.

Fig. 2 PB-10 Sartorius acidometer

Table 2 Mix proportion of the concrete mixtures

Cement /kg/m^3	Sand /kg/m^3	Coarse aggregate /kg/m^3	water /kg/m^3	w/c	w/b	Undisturbed fly ash / kg	Reducing-water agent / kg
450	678	1040	159	0.353	0.304	60.0	12.8

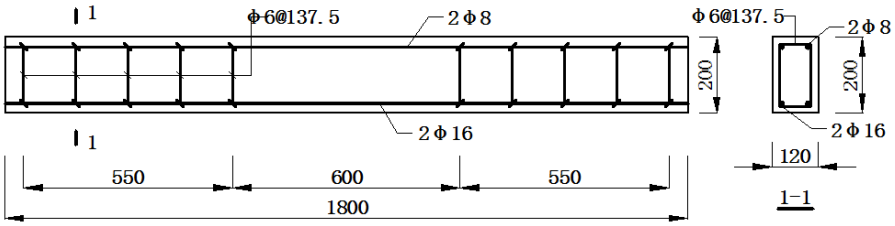

Fig. 3 Configuration of the specimen (unit: mm)

Fig. 4 Specimens immersing in the acid solution

4. Experimental investigation

In this section, damage processes and properties of concrete at different locations, and dynamic and flexural behavior of RC beams subjected to the three accelerated corrosion methods were evaluated.

4.1 Specimen preparation

Eleven RC beams as shown in Fig. 3 were constructed and cured in the natural condition. Commercial concrete was used, with mix details shown in Table 2. The compressive and tensile strengths of reinforcing steel were 210 MPa and 310 MPa, respectively. Strain gauges were bonded to the steel surface to measure the strain of the reinforcing steel.

The specimens were divided into four groups based on the simulated environment that they were subjected to, denoted as series C, S, DW, and I. Series C acted as a control specimen, which was kept in a natural condition. Series S was conditioned in the artificial rainfall by the designed simulator. Series DW was attacked by the wetting-drying cycles. During each cycle, the specimens are immersed in the acid solution for 6 hours and then dried in the natural condition for 18 hours. Series I was immersed in the acid solution (Fig. 4). Table 3 lists details of the specimens. The protocol of the artificial rainfall method was raining six hours continuously per 24 hours. It was estimated that the average rainfall intensity during 20 days was 1,000 mm, which was very close to reported average rainfall amount of 994 mm between January 1, 2010 and May 20, 2010 in Dening City in China.

Table 3 Grouping and corrosion environment

Series	Specimen No.	Damage environment	pH level	Exposure time / day
C	C-0	Controlled	7.0	0
S	S-10	Acid rainfall simulator	1.5	10
	S-20			20
DW	DW-10	wet-dry cycle, immersing 6 hours, drying for 18 hours	1.5	10
	DW-20			20
I1	I1-10	Immersing in the acid solution completely	1.5	10
	I1-20			20
	I1-30			30
I2	I2-10		2.5	10
	I2-20			20
	I2-30			30

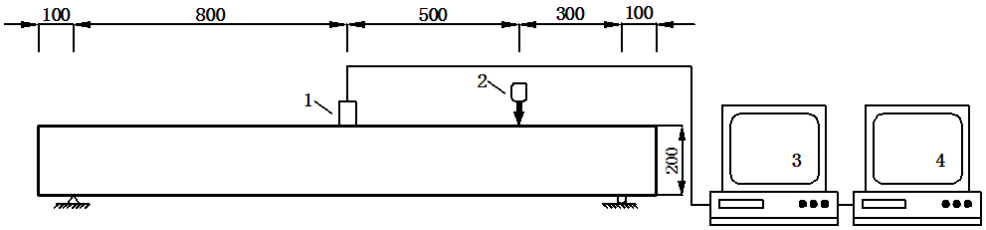

1. Acceleration transducer; 2.Force hammer; 3. Data acquision system; 4. Computer

Fig. 5 Dynamic experiment setup (unit:mm)

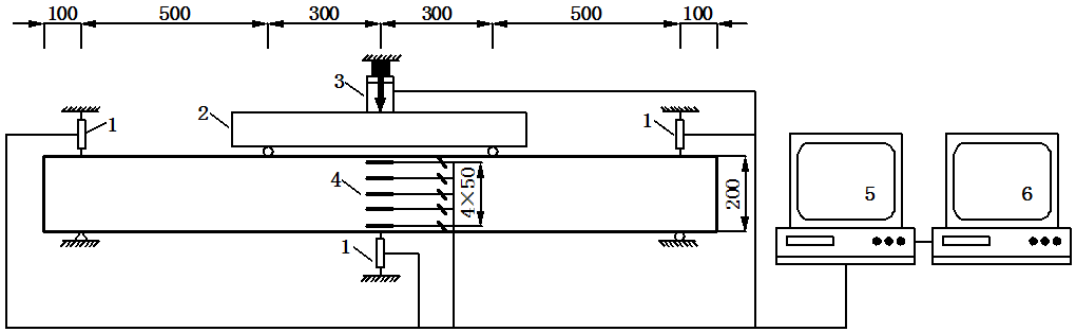

1. Displacement meter; 2. Spreader beam; 3.hydraulic jack; 4. Stain gauge; 5. Data acquision system; 6. Computer

Fig. 6 Loading setup (unit: mm)

4.2 Experimental procedure

After the accelerated corrosion process was completed, a series of nondestructive and destructive tests were performed on the damaged beams. Firstly, ultrasonic technology was applied to evaluate the corrosion depth and compressive strength of the concrete. Since the natural frequency varies with the change of the building materials and servicing environments, dynamics

tests were carried out to examine the integrity of the damaged beams. An acceleration transducer was attached to the surface of the beam. DH3817 dynamic acquisition system with a maximum sampling frequency of 200Hz was used to collect the test data. Based on the principle of wave propagation, knock response method in experimental mechanics was adopted to measure the response of the acceleration transducer (see Fig. 5). Next, three-point bending tests were performed to investigate the flexural behavior of the damaged beams. The experimental setup is shown in Fig. 6. After the bending tests, concrete samples with dimensions of 10 mm×10 mm×10 mm were taken out from the damaged beams, and SEM tests were conducted to evaluate micro properties of concrete under various damage conditions.

5. Results and discussions

5.1 Surface description

During the tests, specimens in different groups behaved differently, as summarized in Table 4 and illustrated in Fig. 14 for crack propagations. Surface evolutions of the concrete beam were recorded during the test, as shown in Fig. 7. It is apparent that as the damage continues, more pores occur and the surfaces become rougher.

5.2 Damage evolution of concrete

5.2.1 Mechanical behavior of concrete.

Ultrasonic technique (Fan *et al*. 2012) was applied to determine the corrosion depth and compressive strength of concrete in this research. The test results are presented in Table 4. Evolutions of corrosion depth and compressive strength of concrete versus exposure time are given in Fig. 8, which indicates that all the three accelerated corrosion methods significantly damaged the concrete. The degree of damage in the descending order is I1, DW, S, and I2. The relationships between corrosion depth and compressive strength of concrete correlate with the results from the authors' previous study (Fan *et al*. 2010).

5.2.2 Micro structure analysis of the concrete

To better understand the evolution of the microstructure of concrete in various parts of the

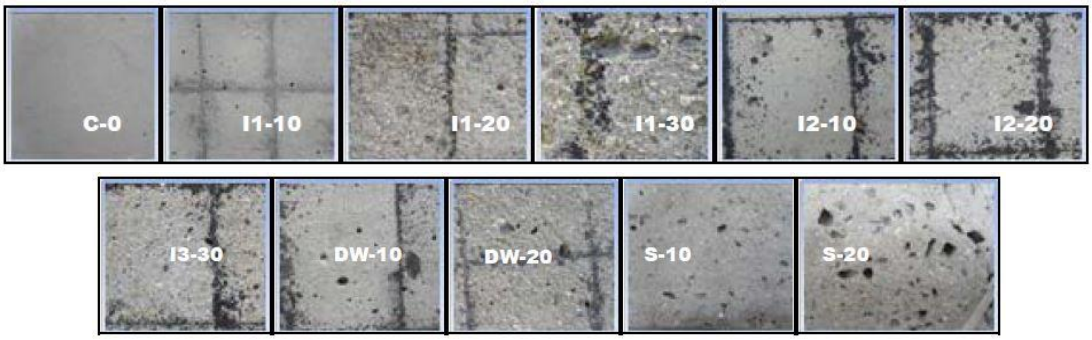

Fig. 7 Concrete surface of the tested beams

Table 4 Testing results of the damage condition of concrete specimens

Series	No.	Damage depth/ mm	Compressive strength/ MPa	Frequency / Hz	Ultimate load / kN	Ultimate displacement / mm
C	C-0	0.0	33.60	44.45	95.8	20.9
S	S-10	17.1	26.67	46.80	94.6	22.1
	S-20	21.5	24.80	49.34	92.6	24.8
DW	DW-10	24.6	31.19	45.62	95.7	22.4
	DW-20	28.7	24.39	45.03	91.4	16.7
I1	I1-10	7.7	25.33	42.29	91.6	18.0
	I1-20	13.4	20.30	45.03	87.7	19.6
	I1-30	50.3	9.20	47.78	84.4	19.0
I2	I2-10	7.3	31.96	44.25	92.3	18.1
	I2-20	11.3	29.70	40.34	90.4	19.2
	I2-30	10.0	27.06	37.19	87.2	21.3

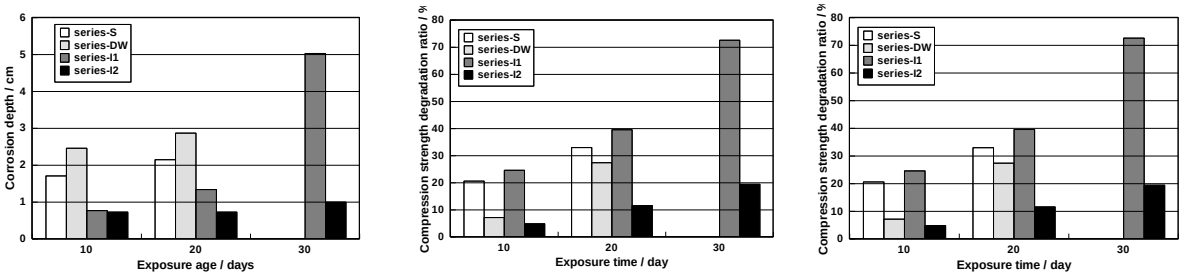

(a) corrosion depth versus time (b) compressive strength versus time (c) corrosion depth versus strength

Fig. 8 Damage evolution of concrete with exposure time

beam, concrete samples with dimensions of 1 cm×1 cm×1cm were obtained from the top (upper surface), center (100 mm from the upper surface) and bottom (bottom surface) of concrete beams of DW-10, DW-20, S-10, and S-20, and evaluated using a JSM-6360LV SEM system. The accelerating voltage of 20kV was applied. Small fractured samples were coated with 5 to 10 nm thick gold to make them conductive.

The microstructures of the concrete samples are shown in Fig. 9. Based on morphology analyses, it is clear that chemical compounds in the concrete have changed. For the S-beams, due to the action of raindrops, the microstructure is quite different along the depth of the beam. More cracks can be observed at the top surface of the S-beams comparing to bottom surface. For the I- and DW-beams, microstructure of the concrete is similar. With the corrosion continued, internal cracks were gradually generated. It is noted that, due to loading effect, some micro cracks can be observed in the concrete samples obtained from the bottom of the beam.

5.3 Structural integrity

Dynamic properties of the damaged beams were evaluated based on the excitation of the beams caused by a force hammer. The 1st natural frequency of the beams is shown in Fig. 10. It is observed that the evolution of the beam frequency is different. While the frequency increases as the corrosion continues for S- and I1- beams, the frequency decreases at the initial damage state

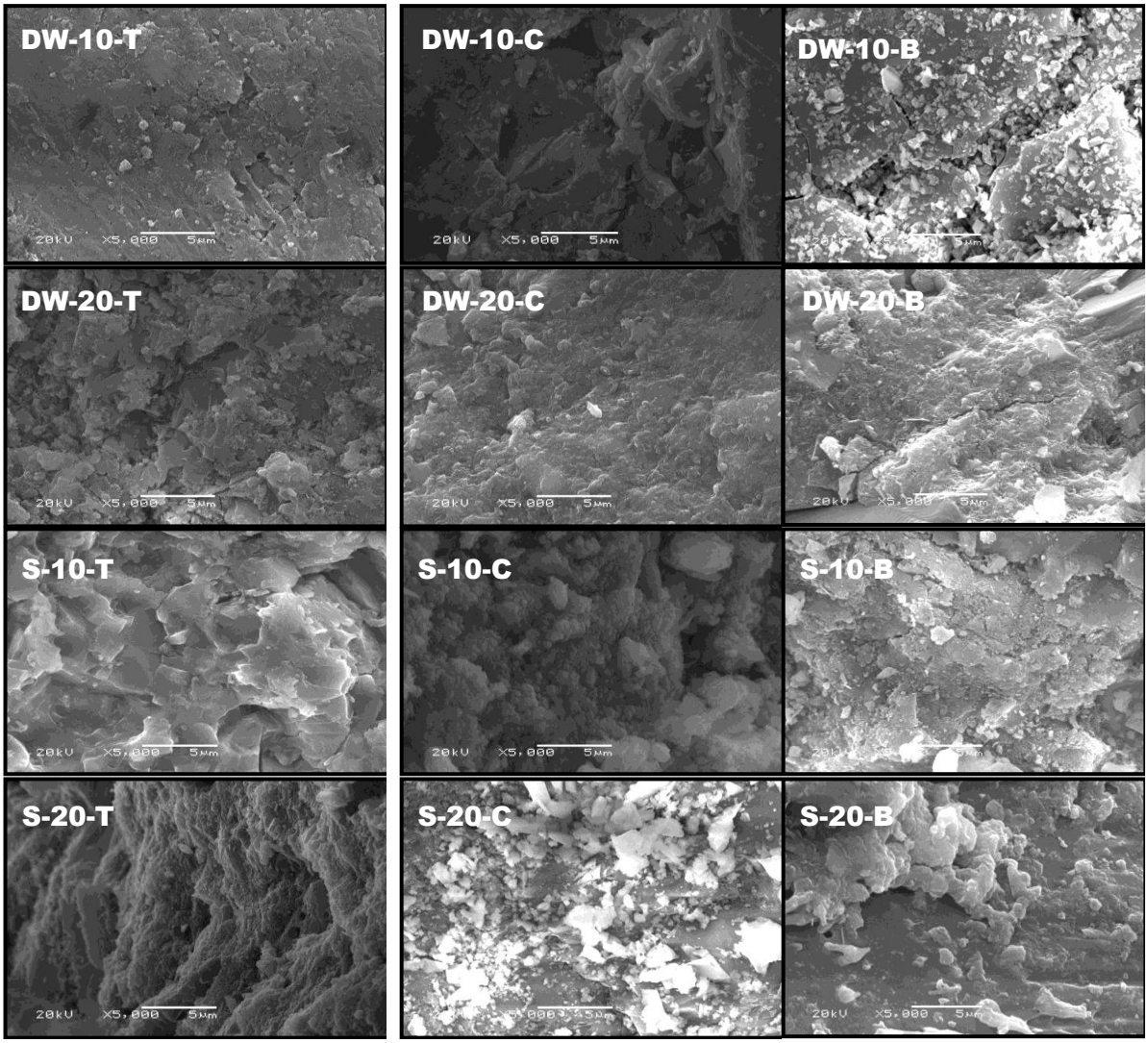

Note: -T,-C, and –B indicate the microstructures obtained from the top, center and bottom of concrete beam

Fig. 9 SEM micrograph of concrete taken out from the RC beams

and then increases for DW- and I2-beams. Therefore, it can be concluded that beam frequency decreases significantly under a severe corrosion environment. However, under a moderate corrosive environment, a short increase of beam integrity occurs at the initial corrosion stage.

5.4 Flexural behavior

Three-point bending tests were performed on the RC beams. Load-deflection curves, cracking progress, cracking and ultimate strength, and failure modes were recorded. The applied load versus the deflection at the center of the beam curves are shown in Fig. 11. The ultimate strength and displacement of the beams are presented in Table 4. Test results obtained by the three accelerated

methods are compared with the controlled specimen in Fig. 12. The failure modes of the specimens are shown in Fig. 13. The crack propagations of the beams are shown in Fig. 14.

As can be seen from Figs. 10 through 12, the effects of the three corrosion methods on the load carrying capacity of the RC beams are: C>S>DW>I2>I1 for bending strength and S>DW>C>I2>I1 for the ultimate displacement. Therefore, both immersion and wetting-drying methods magnify the effect of the real acid rainfall on the RC beams.

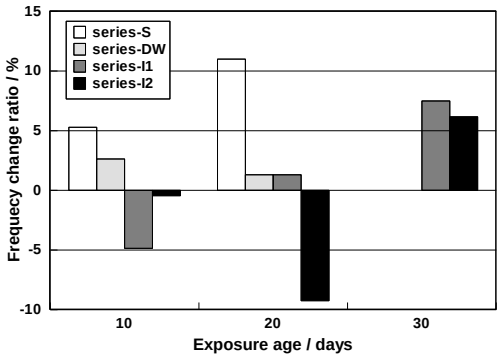

Note: Frequency change ratio = (frequency of the corroded beam-frequency of the beam)/ frequency of the beam

Fig. 10 Frequency versus conditioning age

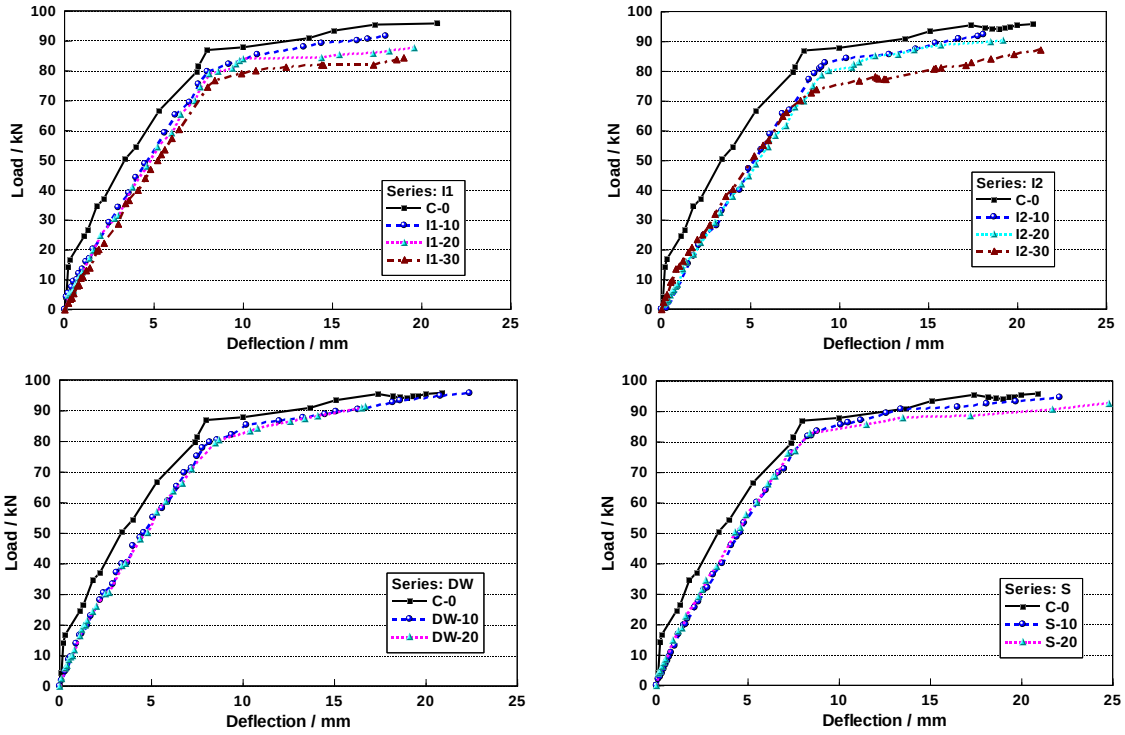

Fig. 11 Applied load versus displacement

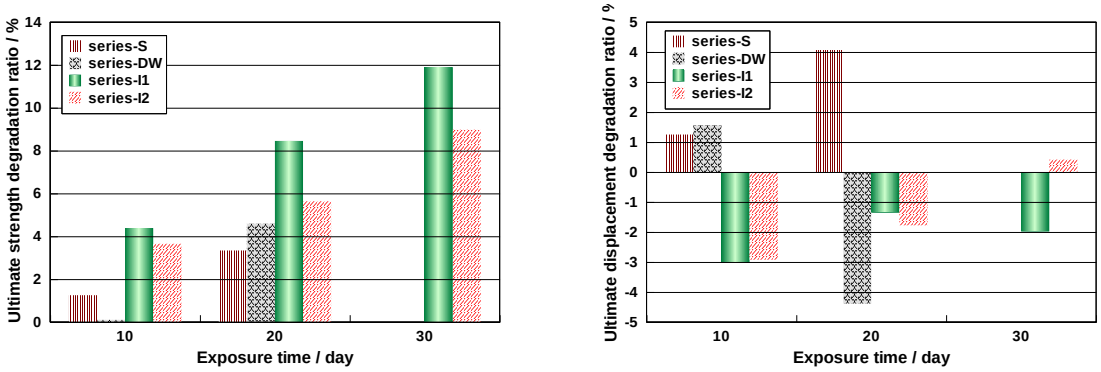

Note: ultimate strength degradation ratio=(ultimate strength of the beam-ultimate strength of the corroded beam)/ultimate strength of the beam; ultimate displacement degradation ratio=(ultimate displacement of the beam-ultimate displacement of the corroded beam)/ultimate displacement of the beam.

Fig. 12 Flexural behavior of the beams under different exposure time

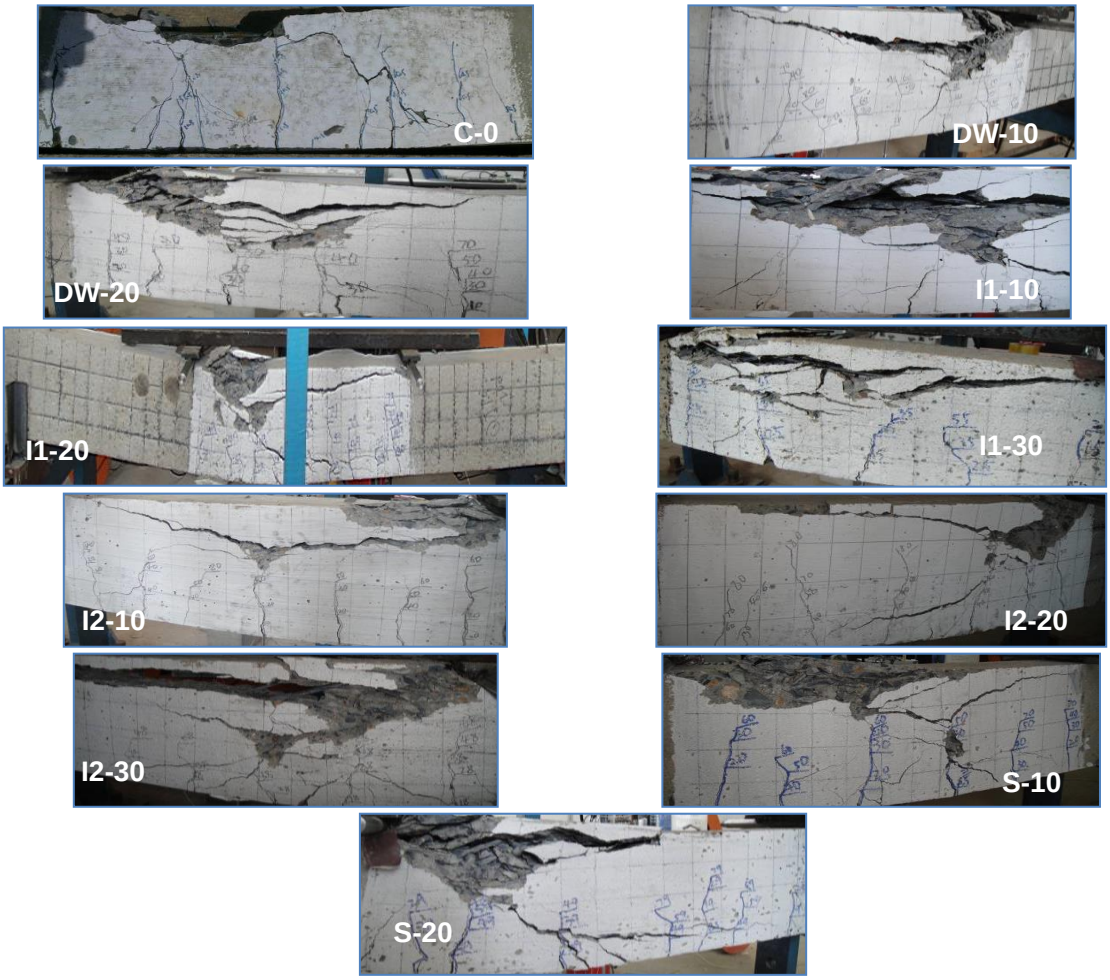

Fig. 13 Failure modes of the reinforced concrete beams

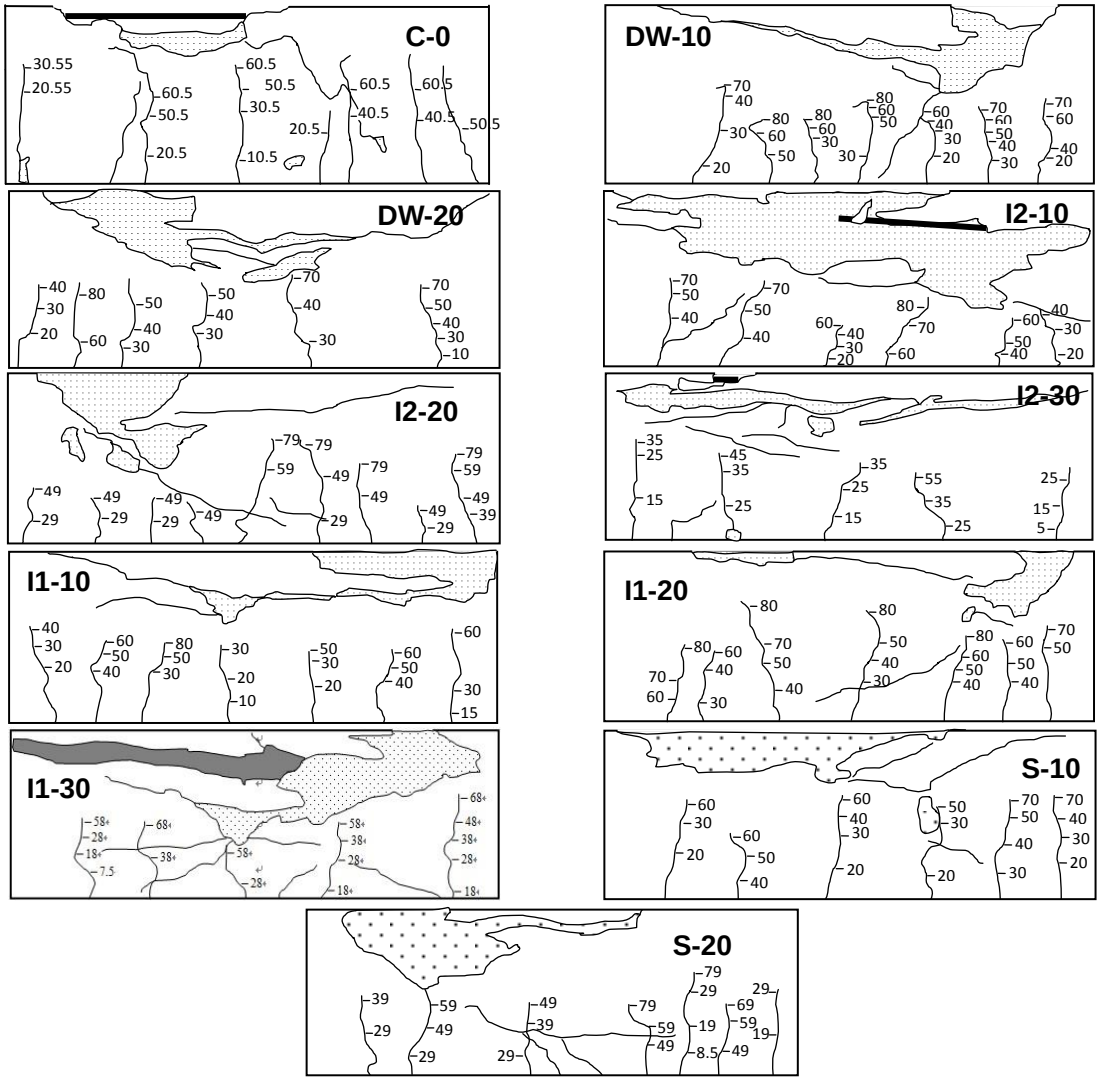

Fig. 14 Cracking propagation process in the bending area of the tested beams (Unit: kN)

6. Conclusions

This study is focused on quantitative evaluations of the effect of acid rain on RC beams. An acid rainfall simulator was designed and evaluated in the laboratory. Three accelerated conditioning tests, including immersion, wetting-drying and rainfall simulator tests, were carried out on ten RC beams. Considering the chemical composition of the acid rain, the acidic solution with pH level of 1.5 and 2.5 were prepared by mixing sulfate and nitric acid solutions. A series of tests, including ultrasonic nondestructive test, compressive strength, SEM, dynamic, and three-point bending tests, were conducted on the concrete and the RC beams exposed to the accelerated environments at specific periods. The effects of the three accelerating corrosion methods on the damage state and flexural behavior of the beams, including corrosion depth,

compressive strength, and microstructure of concrete, flexural strength, ultimate displacement, frequency, failure modes, and crack propagations, were investigated. Based on this study, the following conclusions can be drawn:

• As a major contribution, an acid rain simulator was designed in this study. It was evaluated and proven to more accurately simulate the acid rainfall. A patent has been granted for the designed simulator.

• Three accelerated conditions were simulated in the laboratory and can effectively deteriorate the concrete, but at different rates. The compressive strengths and damage depths resulting from the three corrosion methods in the descending order are I1, S, DW, I2; and DW, S, I1, I2, respectively. The relationship between the corrosion depth and compressive strength is approximately linear.

• Micro structure of the concrete samples obtained from the top, center and bottom parts of the beam were examined using SEM analyses. The SEM micrograph can well explain the macro behavior of the concrete. Based on both macro and micro analyses, it can be concluded that various exposure methods results in varying degrees of degradation.

• The beam frequency varies with the damage states of the beams. It was observed that the 1st frequency of the beams from series S and I1 increases as the corrosion continues. For the beams from series DW and I2, the frequency decreases slightly and then increases. It can be concluded that more severe servicing environment decreases the beam integrity more significantly. Under a moderate corrosive environment, the beam integrity will have a short increase at the initial corrosion stage.

• Based on the results from three-point bending tests conducted on the RC beams damaged by the three accelerating methods, the ultimate strength and displacement in the descending order are C, S, DW, I2, I1; and S, DW, C, I2, I1, respectively. It is illustrated that the flexural strength and ultimate displacement of S-beams are better than those from the other three series of beams. Therefore, both immersion and wetting-drying methods magnify the action of real acid rain on the concrete beams.

Acknowledgements

This research was financially supported by the National Natural Science Foundation of China (Grant No. 51178069), National Natural Science Foundation of China (Grant No. 50708010), the Program for New Century Excellent Talents in University (Grant No.NCET-11-0860), and the Liaoning Provincial Fund for Distinguished Yong Scholars.

References

Ababneh, A. and Sheban, M. (2011), "Impact of mechanical loading on the corrosion of steel reinforcement in concrete structures", *Mater. Struct.*, **44**, 1123-1137.

Belie, D.N., Monteny, J. and Taerwe, L. (2002). "Apparatus for accelerated degradation testing of concrete specimens", *Mater. Struct.*, **35**(251), 427-433.

Berner, E.K. and Berner, R.A. (1996), *Global environment: water, air and geochemical cycles*, Prentice Hall, New Jersey, USA.

Chen, M., Wang, K. and Xie, L. (2013), "Deterioration mechanism of cementitious materials under acid rain attack", *Eng. Fail. Anal.*, **27**, 272-285.

Eney, A.B. and Petzold, D.E. (1987), "The Problem of acid rain: an overview", *Environ.*, **7**(2), 95-103.
Fan, R.S. and Lee, Z.B. (1991), "Artificial rainfall device for soil erosion study", *Acta Conservations Soil et Aquae Sinica*, **5**(2), 38-45. (in Chinese)
Fan, Y. and Zhang, S. (2012), One kind of artificial rainfall simulator, Patent ZL201220079096.1, China.
Fan, Y., Hu, Z., Zhang, Y. and Liu, J. (2010), "Deterioration of compressive property of concrete under simulated acid rain environment", *Construct. Build. Mater.*, **24**, 1975-1983.
Fan, Y., Hu, Z. and Liu, J. (2012), "Ultrasonic measurement of corrosion depth development in concrete exposed to acidic environment", *Int. J. Corros.*, Article ID 749185, doi:10.1155/2012/749185.
Fan, Y., Hu, Z. and Luan, H. (2012), "Deterioration of tensile behavior of concrete exposed to artificial acid rain environment", *Interact. Multis. Mech.*, **5**(1), 41-56.
Fan, Y., Zhou, J. and Hu, Z. (2005), "Application of fractals to study the corroded reinforced concrete beam", *Struct. Eng. Mech.*, **20**(3), 265-277.
Francois, R., Khan, I. and Dang, V.H. (2013), "Impact of corrosion on mechanical properties of steel embedded in 27-year-old corroded reinforced concrete beams", *Mater. Struct.*, **46**, 899-910.
Grismer, M. (2012), "Standards vary in studies using rainfall simulators to evaluate erosion", *Calif. Agriculat.*, **66**(3), 102-107.
Keller, E.A. (2012), *Introduction to environmental geology*, Prentice Hall, New Jersey, USA.
Laws, J.O. (1941), "Measurements of the fall-velocity of water-drops and raindrops", *Tran., Am. Geophys. Uni.*, **22**, 709-720.
Larssen, T., Seip, H.M., Semb, A., Mulder, J., Muniz, I.P., Vogt, R. D., Lydersen, E., Angell, V., Dagang, T. and Eilertsen, O. (1999), "Acid deposition and its effects in China: an overview", *Environ. Sci. Policy*, **2**, 9-24.
Mansfeld, F. and Vijayakumar, R. (1988), "Atmospheric corrosion behavior in Southern California", *Corros. Sci.*, **28**(9), 939-946.
Neuman, K. (1985), "Trends in public opinion on acid rain: a comprehensive review of existing data", *Water, Air, Soil Pollut.*, **31**(3-4), 1047-1059.
Okochi, H., Kameda, H., Hasegawa, S., Saito, N., Kubota, K. and Igawa, M. (2000), "Deterioration of concrete structures by acid deposition-an assessment of the role of rainwater on deterioration by laboratory and field exposure experiments using mortar specimens", *Atmosph. Environ.*, **34**, 2937-2945.
O'Flaherty, F.J., Mangat, P.S., Lambert, P. and Browne, E.H. (2008), "Effect of under-reinforcement on the flexural strength of corroded beams", *Mater. Struct.*, **41**, 311-321.
Park, S.W., Mitchell, J.K. and Bubenzern, G.D. (1987), "Rainfall characteristics and their relation to splash erosion", *Tran. ASABE*, **26**(3), 795-804.
Sangüesa, C., Arumi, J., Pizarro, R. and Link, O. (2010), "A rainfall simulator for the in situ study of superficial runoff and soil erosion", *Chil. J. Agricult. Res.*, **70**(1), 178-182.
Singh, A. and Agrawal, M. (2008), "Acid rain and its ecological consequences", *J. Environ. Biology*, **29**(1), 15-24.
Xie, S., Qi, L. and Zhou, D. (2004), "Investigation of the effects of acid rain on the deterioration of cement concrete using accelerated tests established in laboratory", *Atmosph. Environ.*, **38**, 4457-4466.
Xu, X.Z., Liu, D.Q. and Zhang, H.W. (2006), "Laboratory rainfall simulation with controlled rainfall intensity and drainage", *J. Beijing Forest. Univ.*, **5**, 53-58.
Xie, S., Qi, L. and Zhou, D. (2004), "Investigation of the effects of acid rain on the deterioration of cement concrete using accelerated tests established in laboratory", *Atmosph. Environ.*, **38**, 4457-4466.
Zhao, Y.X. (2006), "Spatial-temporal distribution of acid rain in China during 2005", *Adv. Clim. Change Res.*, **2**(5), 242-245.
Zhang, X., Chai, F., Wang, S., Sun, X. and Han, M. (2010), "Research progress of acid precipitation in China", *Res. Environ. Sci.*, **5**, 527-532. (in Chinese)
Zhang, X., Jiang, H., Jin, J., Xu, X. and Zhang, Q. (2012), "Analysis of acid rain patterns in northeastern China using a decision tree method", *Atmosph. Environ.*, **46**, 590-596.
Zhou, J., Chen, X. and Chen, S. (2011), "Durability and service life prediction of GFRP bars embedded in concrete under acid environment", *Nucl. Eng. Des.*, **241**, 4095-4102.